Soldagem & Inspeção

ISSN 1980-6973 (Online) | ISSN 0104-9224 (Print)
TECHNICAL PAPERS

# Comparison of Aluminum Based Alloys Reinforced with Intermetallic Developed by Powder Metallurgy and Arc Melting Routes

Syeda Ammara Batool[1], Abdul Wadood[1], Muhammad Atiq Ur Rehman[1]

[1] Institute of Space Technology Islamabad, Department of Materials Science and Engineering, Islamabad, Pakistan.

**How to cite:** Batool SA, Wadood A, Rehman MAU. Comparison of aluminum based alloys reinforced with intermetallic developed by powder metallurgy and arc melting routes. Soldagem & Inspeção. 2019;24:e2419. https://doi.org/10.1590/0104-9224/SI24.19

**Abstract:** In this work, Al-Ti alloys were prepared using metallic powders of Al and Ti via Powder Metallurgy (PM) and Arc Melting (AM) route. Four chemical compositions including pure aluminum were studied. Metallic powders were mixed with three compositions, Al-5Ti, Al-10Ti and Al-10Ti-2SiC. All the compositions were in atomic percentage. In case of PM, samples were pressed uniaxially at 170 MPa to fabricate 10 mm diameter compacts followed by pressure-less sintering at 620°C under argon atmosphere for 4 hr. Pure Al showed densification up to 96% whereas sample with 5 at.% Ti decreased in densification to 90%. For samples with 10 at.% of Ti and with 2 at.% SiC, densification values were 92% and 93%, respectively. In the case of AM method, the process was carried out under vacuum in Argon atmosphere followed by homogenization at 600°C for 1 hr. The resulting microstructure and composition of samples were analyzed. X-ray diffraction (XRD) results confirmed the formation of $TiAl_3$ intermetallic phase in the alloy. The mechanical test used to assess samples performance was hardness. Hardness results showed a strong increase in hardness with increasing Ti contents and SiC addition for both types of samples. The developed Al-Ti and Al-Ti-SiC alloy exhibit better hardness properties and have the potential to be used for light-weight materials applications.

**Key-words:** Arc melting; Powder metallurgy; Intermetallics; Phase constitution.

## 1. Introduction

Aluminum (Al, 2.7 g/cm$^3$) and Titanium (Ti, 4.5 g/cm$^3$) both are low-density materials as compared to steel (7.8 g/cm$^3$) and possess high specific strength [1-3]. Al and Ti form passive oxide layers in the atmosphere which results in the good corrosion resistance [4].

Aluminum-based lightweight materials is a topic of interest among scientists and engineers working in the transportation industry especially in the aerospace industry. Reduced weights of vehicles improve fuel efficiency. Mostly used lightweight materials for structural applications are Aluminum (Al), Magnesium (Mg), Titanium (Ti), Beryllium (Be), Titanium Aluminides, Engineered Plastics, Structural Ceramics, Metal Matrix Composites (MMCs), Polymer Matrix Composites (PMCs) and Ceramic Matrix Composites (CMCs) [3,5]. Tisza and Czinege [6] compared the application of light-weight Aluminum with heavy-weight steel in the production of automotive parts. Campbell [3] provides the uses of lightweight materials in details. Apart from structural utilities, light-weight materials including Aluminum alloys are widely being used in sports applications [7], power generation plants [8] and body implants [9].

Intermetallic compounds (IMCs) are ordered compounds comprising of two or more than two elements in a fixed ratio having a complex crystal structure different from the parent elements. These elements can be metals or combination of metals and non-metals. Mixed bonding is present in Intermetallics i.e. partially covalent/ionic and partially metallic [10]. Their most attractive properties are low density, high strength, high creep and corrosion resistance at elevated temperatures [11-13]. However, some disadvantages e.g. low ductility, high brittleness, low fracture toughness, difficulties in fabrication and post-fabrication machining, etc. are also associated with Intermetallic compounds which limits their structural applications [14,15].

Al-Ti binary system produces different intermetallic compounds (IMCs) at different compositions of Al and Ti. With the varying composition of Ti in Al metal, alloys of different physical and mechanical properties are produced. Different IMCs known as Titanium Aluminides (Ti-Aluminides) formed in the Al-Ti system are $Ti_3Al$, TiAl (δ phase), $Ti_2Al_5$, $TiAl_2$ and $TiAl_3$ [16]. The solid solubility of Ti in Al is limited i.e. less than 0.7 atomic% (1.3 weight %), so mechanical properties of these alloys mildly get influence by solid solution strengthening [17]. Due to the limited solubility of Ti in Al, the major strengthening effect is caused by Intermetallics produced in this system which act as precipitates dispersed in alloy matrix, enhancing mechanical aspects of the alloys. Al-Ti alloys show a

Received: 05 Mar., 2019. Accepted: 08 July, 2019.
E-mails: syedaammara001@gmail.com (SAB), wadood91@gmail.com (AW), muhammad.atiq@ist.edu.pk (MAUR)

combination of better physical and structural properties than individual Al and Ti metals. These alloys are lightweight, possess high strength to weight ratio and capable of operating at high temperatures [16,17].

Alloys based on Al-Ti Intermetallics impose difficulties in processing because of their low ductility and high brittleness at room temperature. Desirable properties of these alloys were not achievable in the past due to the lack in understanding of their microstructure and the deformation mechanism. Influence of gamma titanium aluminides is given in Kim [18] and Liu et al. [19]. is related to the tensile properties and fracture toughness of TiAl alloys with controlled microstructures. Microstructure stability and the creep properties of intermetallic β-solidifying γ-TiAl based alloys is given in Kastenhuber et al. [20]. Review on improvements in the surface performance of TiAl-based alloys by double glow plasma surface alloying technology is given in Lin et al. [21]. With the advancement in the manufacturing techniques, deep knowledge of the microstructure-property relationship, and the influence of alloying elements. has led to the industrial scale production of Al-Ti Intermetallics based alloys [22-24]. Proper heat treatment of these alloys results in the refined grain structure which in turn improves room temperature ductility. Among the Intermetallics produced in Al-Ti binary system, $TiAl_3$ have the lowest density (3.4 g/cm$^3$), highest micro hardness value (465-670 kg/mm$^2$) and best oxidation resistance [25]. However, high brittleness renders its deployment for aerospace and other light weight applications. Processing technologies resulting in near-net shape are so far considered the best option for manufacturing these Intermetallics to avoid numerous processing and post-processing steps [25]. These techniques include sintering from metallic powders, arc melting, direct metal deposition, laser forming etc. Development of freeform fabrication method for Ti-Al-Ni intermetallics is given in Cao et al. [26]. In situ formation of Ti-TiAl Intermetallic composite by electric current activated sintering method is explained in detail in Yener et al. [27] and Yue et al. [28] discusses the combustion synthesis of γ-TiAl Intermetallic compound.

The processing techniques used in this research are based on sintering of metallic Al-Ti compact and arc melting of Al-Ti powder compacts using button arc furnace. The composition of powders is chosen in order to produce alloys of rich Al content i.e. Al-5Ti, Al-10Ti, and Al-10Ti-2SiC are mixed together. Comparison of the properties of aluminum-titanium based alloys with and without ceramic reinforcement SiC is also presented. Composition range selected for this research was 5-10 atomic % addition of Ti in Al. In the Al-Ti binary system, this composition falls in the range of intermetallic compound $TiAl_3$ [20]. A small amount (2 atomic%) of SiC powder was also added in one sample to observe the effect of ceramic reinforcement in the developed Al-Ti alloy.

## 2. Experimental Work

The particle size of powders was analyzed using a laser diffraction particle size analyzer. Powder morphology was evaluated using field emission Scanning electron microscope. Four sample mixtures were prepared. Pure Al sample was prepared as a reference. Metallic powders were mixed with three atomic compositions, Al-5Ti, Al-10Ti, and Al-10Ti-2SiC. All powder mixtures were subjected to dry milling in a Cole-Palmer (Model: RZ-04149-05) ball mill prior to compression to ensure uniform mixing of metal powders. The milling time was 3 hours at a rotational speed of 100 rpm. Zirconia balls were used as grinding medium. Media-to-powder ratio was kept as 3:1. Compaction of powder mixture was performed in a hydraulic press (Specac Hydraulic Press) under a pressure of 170 MPa. Steel die having an internal diameter of 10 mm was used for pressing. Holding time of the press was kept for 3 minutes for all samples.

### 2.1. Processing via powder metallurgy

The first batch of samples was fabricated by pressure-less solid state sintering. Pellets having a diameter of 10 mm were sintered at 620 °C in a tube furnace (KJ-1600VF, Kejia Furnace Company, China) under argon atmosphere. Uniform heating rate of 5 °C/min was established. Holding time was 4 hrs, followed by room temperature cooling. Annealing of sintered pellets in a chamber furnace (ENTECH Furnace, Sweden) was performed at 160 °C for 7 hrs.

### 2.2. Processing via arc melting

The second batch of samples was fabricated through arc melting. The process was carried out in Edmund Buehler Mini Arc Melter available in the GIK Institute, Pakistan under vacuum. Argon was used as purging gas. The electric arc was generated by non-consumable Tungsten electrode. The current intensity was kept at 80-100 amperes. Titanium getter was used and was melted first to absorb any gases e.g. oxygen to avoid oxidation of metal melt. Samples were then subjected to homogenization in the tube furnace at 600 °C for about 1 hr. Alloy samples of pure Al, Al-5Ti, Al-10Ti, and Al-10Ti-2SiC prepared by powder metallurgy route are shown in Figure 1.

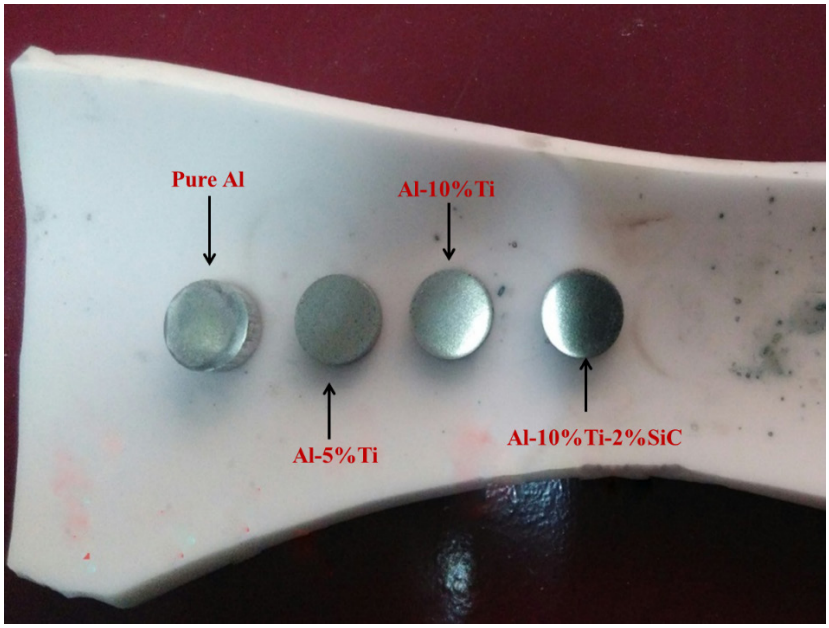


**Figure 1.** Alloy samples of pure Al, Al-5Ti, Al-10Ti and Al-10Ti-2SiC prepared by powder metallurgy route.

### 2.3. Characterization

The density of the alloy samples processed through powder metallurgy was calculated before and after sintering. Green compacts and sintered pellets were weighed using a microbalance and micrometer screw gauge was used to measure thickness and diameter of pellets. Density and percentage densification was then calculated.

Theoretical ρ of all the samples was calculated using the rule of the mixture as shown in Equation 1. The density of Al, Ti and SiC were taken as 2.7, 4.5 and 3.2 g/cm$^3$, respectively.

$$Theoretical\ \rho = \left(\rho_{Al} x\ atom\ \%Al\right) + \left(\rho_{Ti} x\ atom\ \%Ti\right) + \left(\rho_{SiC} x\ atom\ \%SiC\right) \quad (1)$$

For microstructural analysis, samples were prepared according to standard metallurgical procedures. After grinding and polishing with alumina paste, etching of the specimens was done using freshly prepared Keller's reagent (190 mL distilled water with 5 mL $HNO_3$, 2 mL HF, and 3 mL HCl) with immersion time of 30 s. Microstructures of sintered and arc melted Al-Ti alloy samples were evaluated using field emission scanning electron microscope (SEM). For chemical composition, energy dispersive X-ray spectroscopy (EDS) was employed. X-ray diffraction (XRD) was performed to confirm the development of intermetallic phase in the alloy using Cu-Kα (1.5418 °A) radiation in the diffraction angle (2θ) range of 30°-80° with a step size of 0.05. Hardness was measured using micro Vickers hardness testing (Fujitsu HmV-G, Shimadzu Corporation) under a test load of 500g. To obtain an average hardness value, five to seven values were taken for each specimen under the same test load. The complete experimental plan for both powder metallurgy route and arc melting process and the materials characterization techniques carried out in this study is schematically represented in Figure 2.

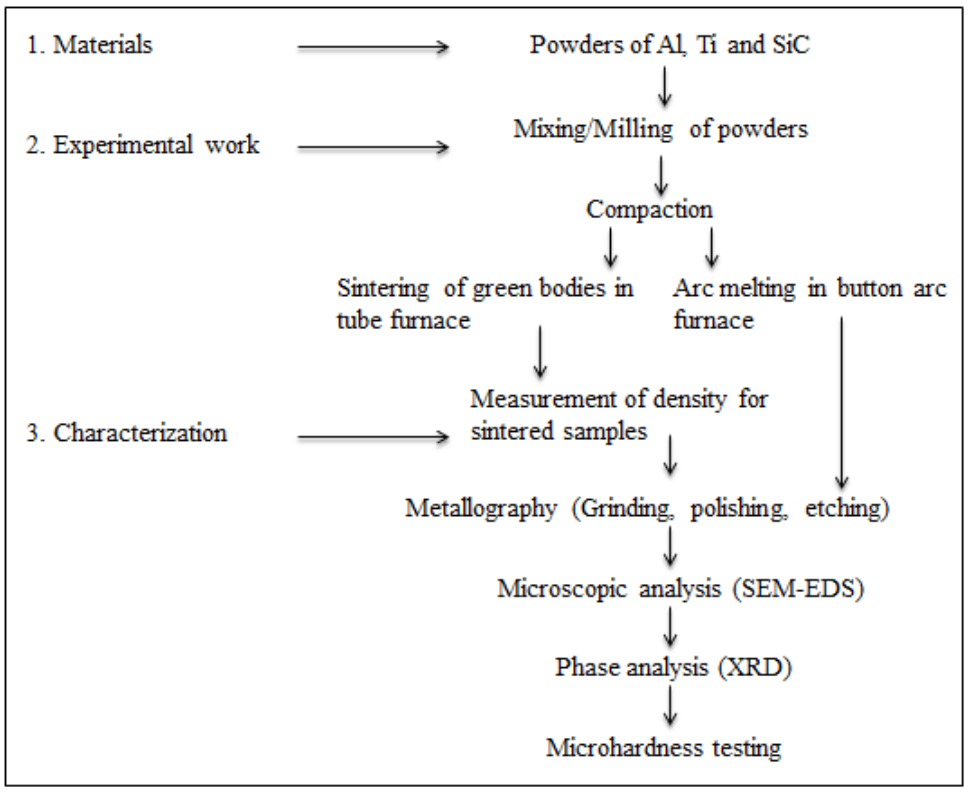


**Figure 2.** Flow diagram of experimental procedures.

## 3. Results and Discussion

### 3.1. Density measurements

Figure 3 shows the SEM micrographs of Aluminum, Titanium and Silicon Carbide powder particles and particle size distribution of these powders using particle size analysis are shown in this Figure as well. The particle size of Aluminum (density 2.7 g/cm$^3$) powder measured by particle size analyzer was 70µm and from SEM it was analyzed that the particles were irregular in shape. It was also analyzed from the SEM micrograph of Figure 3b, the titanium (density 4.5g/cm$^3$) powder used in this study was a porous and irregular shape with a particle size of 100 µm. Dense and irregular shape SiC powder was used as ceramic reinforcement in an intermetallic based alloy having an average particle size of 25 µm. Dimensions (weight, thickness, and volume) of sintered alloy samples along with the theoretical density and resulting densification was measured for alloy compositions developed by powder metallurgy route.

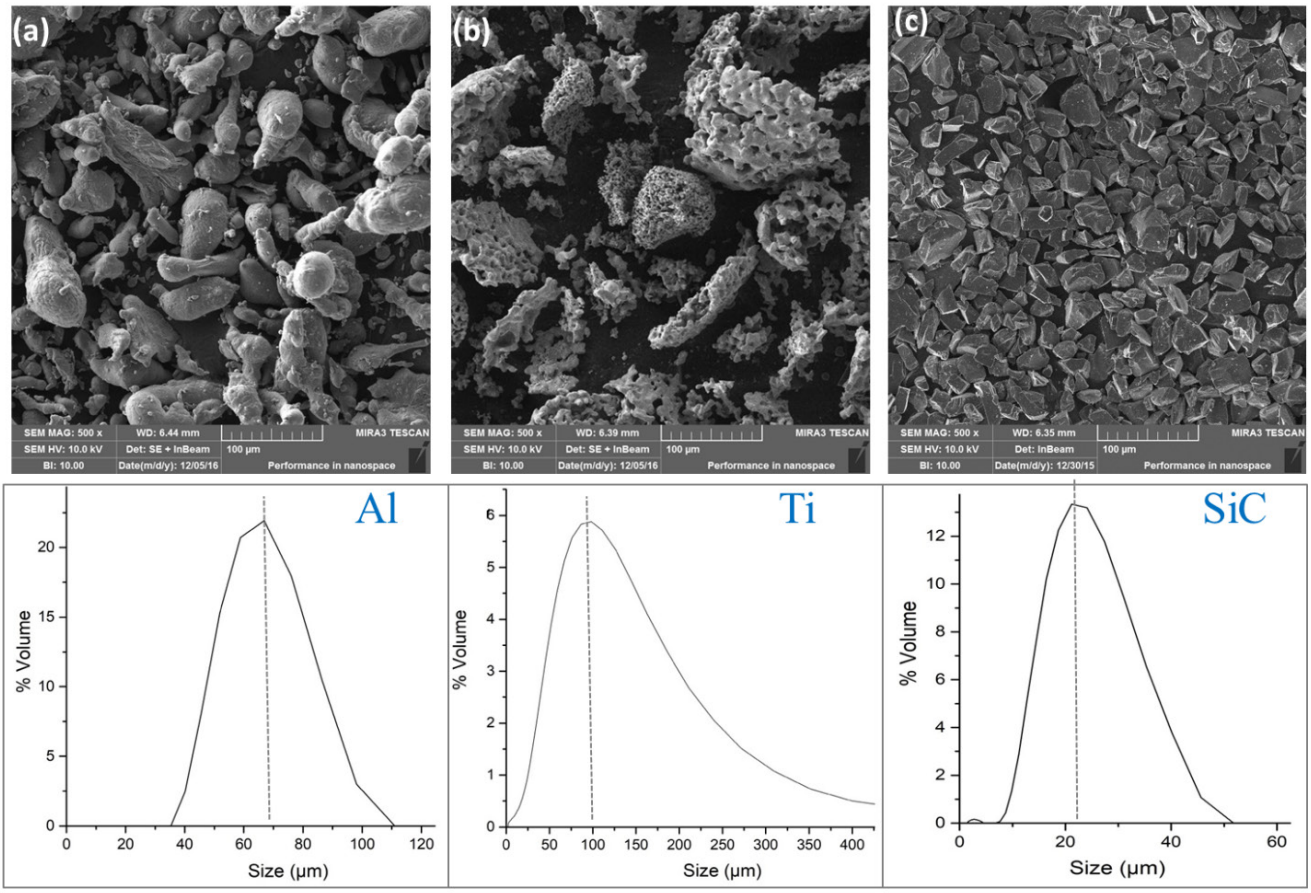


**Figure 3.** SEM micrographs of (a) Al Powder (b) Ti Powder (c) SiC Powder. Particle size distribution is shown below each figure.

The diameter of all the samples was about 10mm as the steel die used for compaction had an internal diameter of 10mm. Densification of developed alloys with composition change is shown in Figure 4.

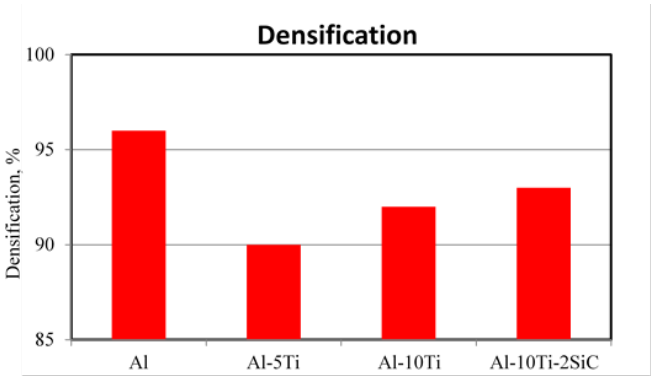


**Figure 4.** Percentage densification variation with composition.

Reasonable densification of 96% was found in pure Al sample. Sample with 5% and 10% Ti addition showed the densification of up to 90% and 92%, respectively. Sample with 2%SiC addition was dense up to 93%. 100% densification was not obtained in any sintered alloy sample. One reason is the fact that Ti powder particles used in the study had spongy shape and all the spaces were not filled leaving some porosity in the sintered samples. Although Al powder used in this study was dense, however even Aluminum did not present 100% densification. This showed that both the process and the porous powders seem to account for the porosity. Although Aluminum and SiC powders used in this study were compact, however, they were irregular in shape, so some porosity remained between these powder particles and 100% densification could not achieve.

### 3.2. SEM-EDS analysis

SEM micrographs of sintered and arc melted alloy samples are shown in Figure 5 and Figure 6 respectively. A contrast of dark and light gray regions can be seen in the samples. The intermetallic phase was observed to be uniformly dispersed in the Al matrix for all samples.

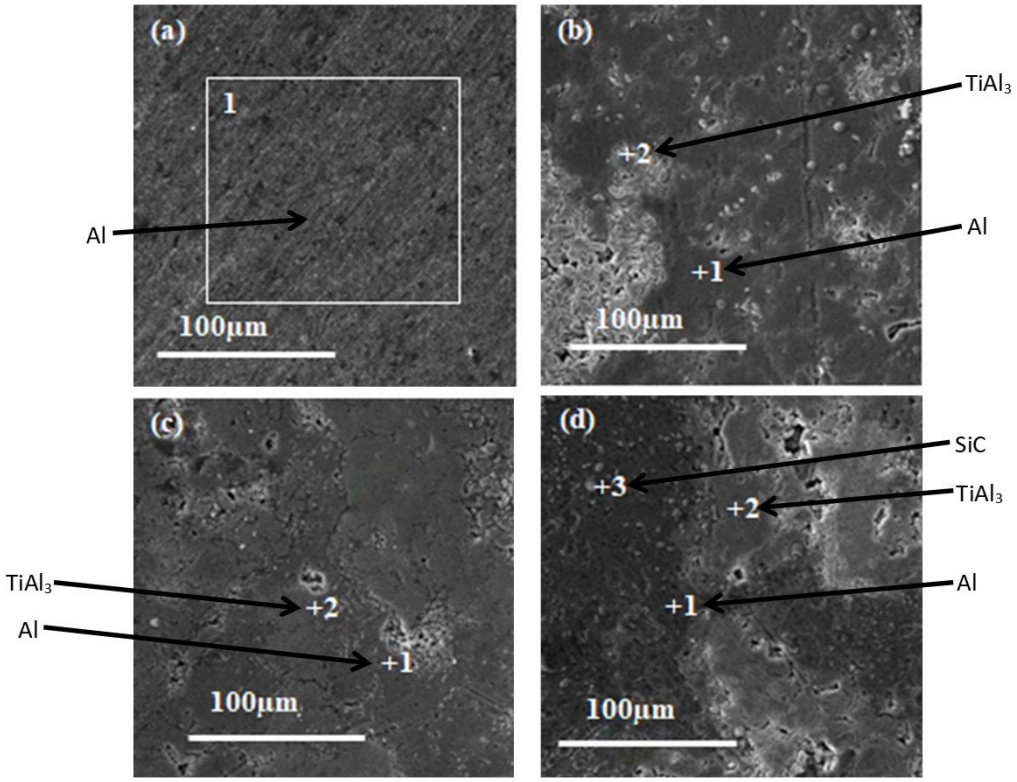


**Figure 5.** SEM-EDX analysis of sintered samples: (a) Pure Al; (b) Al-5Ti; (c) Al-10Ti; (d) Al-10Ti-2SiC.

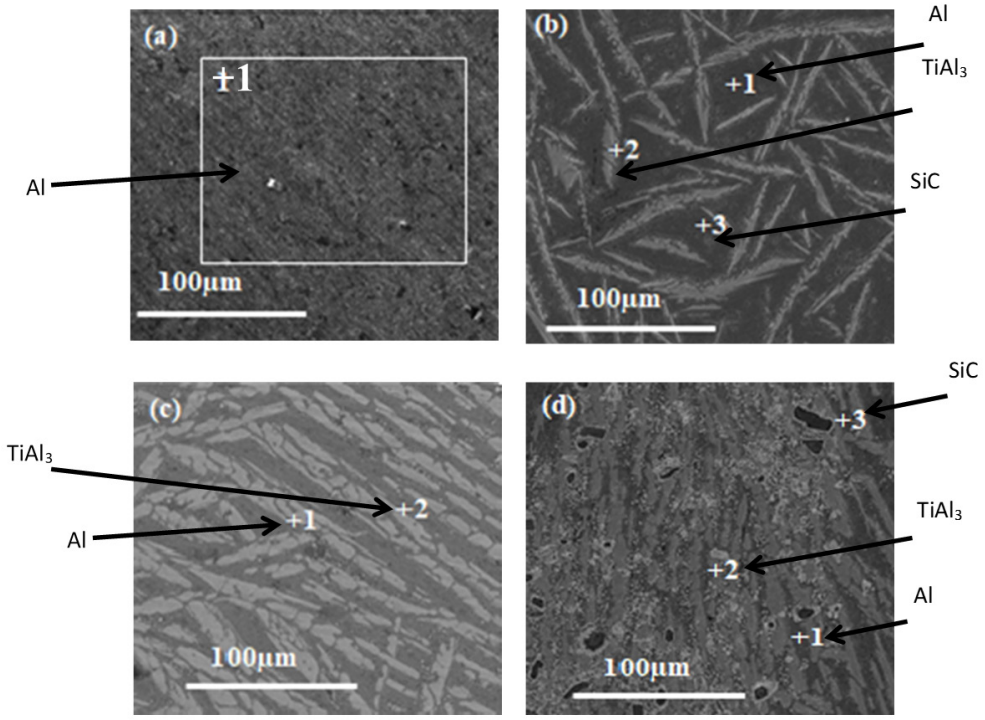


**Figure 6.** SEM-EDX analysis of arc melted samples: (a) Pure Al; (b) Al-5Ti; (c) Al-10Ti; (d) Al-10Ti-2SiC.

Chemical composition of different phases of sintered samples is given in Table 1. SEM-EDX analysis revealed dark regions as pure Al and light regions as intermetallic phase $TiAl_3$. Table 1 (sintered samples) and Table 2 (arc melted samples) give a detailed compositional analysis of different points in the alloy.

**Table 1.** Composition analysis of sintered alloy samples.

| Sample points | (a) Pure Al | (b) Al+5Ti | | (c) Al+10Ti | | (d) Al+10Ti+2SiC | | | | Phase identified |
|---|---|---|---|---|---|---|---|---|---|---|
| | Al | Al | Ti | Al | Ti | Al | Ti | Si | C | |
| +1 | 100 | 100 | 0 | 100 | 0 | 100 | 0 | 0 | 0 | Al |
| +2 | - | 74.86 | 25.14 | 72.21 | 27.79 | 75.41 | 24.59 | 0 | 0 | $TiAl_3$ |
| +3 | - | - | - | - | - | 3.83 | 0.07 | 44.74 | 51.36 | SiC |

**Table 2.** Composition analysis of arc melted samples.

| Sample points | (a) Pure Al | (b) Al+5%Ti | | (c) Al+10%Ti | | (d) Al+10%Ti+2% SiC | | | | Phase identified |
|---|---|---|---|---|---|---|---|---|---|---|
| | Al | Al | Ti | Al | Ti | Al | Ti | Si | C | |
| +1 | 100 | 100 | 0 | 100 | 0 | 100 | 0 | 0 | 0 | Al |
| +2 | - | 75.9 | 24.1 | 75.0 | 25.0 | 73.4 | 26.6 | 0 | 0 | $TiAl_3$ |
| +3 | - | - | - | - | - | 4.9 | 0.9 | 42.6 | 51.6 | SiC |

In Figures 5a and 6a, area analysis was performed which corresponded to 100% Al in both type of samples. No other phases were found. Figures 5b-d and 6b-d shows point analysis. Different phases are shown with arrow heads in these Figures. Point 1 in all samples corresponded to pure Al whereas point 2 showed compositions corresponding to $TiAl_3$ intermetallic phase. Point 3 in Figure 5d and 6d represent SiC. As the Ti amount was increased in samples b and c from 5atomic% to 10atomic%, respectively, the amount of intermetallic phase $TiAl_3$ was observed to increase in Al-10Ti sample as compared to Al-5Ti sample. Figure 6b-d shows uniformly dispersed intermetallic phase in the form of dendrites in the Al matrix oriented in different directions. Comparing these images with the images of sintered samples shown in Figure 5b-d it was observed that intermetallic phase $TiAl_3$ formed in arc melted alloy was more uniformly dispersed in the metal matrix than the intermetallic phase formed in sintered alloy samples. This is related to uniform mixing during arc melting process as compared to solid-state processing in the sintering process. As shown in Figure 6c, SiC particles were dispersed in Aluminum matrix in Al-10Ti-2SiC sample.

### 3.3. Phase analysis (XRD)

Phase analysis of sintered and arc melted alloy samples are shown in Figures 7 and 8 respectively. Pure Al sample (a) was used as a reference. After processing, the formation of intermetallic phase was anticipated. Enough number of peaks of $TiAl_3$ phase was observed in XRD pattern which confirmed the formation of intermetallic phase $TiAl_3$ in Ti added Al-Ti alloy samples. Different peaks were indexed in Figure 7 and Figure 8 for sintered and arc melted alloy samples. SiC phase peak was not clearly analyzed from these XRD diffraction patterns due to the low concentration of SiC in Al-10Ti-2SiC. Only one small peak of $TiAl_3$ phase was identified for Al-5Ti arc melted sample however more than one peaks of $TiAl_3$ phase were clearly identified for sintered Al-5Ti sample. As arc melted samples were uniformly mixed (Figure 6) as compared to sintered samples (Figure 5), so in some regions of sintered Al-5Ti sample, $TiAl_3$ phase was formed. However, in the arc melted Al-5Ti sample, percentage of $TiAl_3$ phase was so small that it could not be detected by XRD.The $TiAl_3$ phase was clearly identified for both sintered and arc melted Al-10Ti and Al-10Ti-2SiC samples.$TiAl_3$ phase peak intensity was also found higher for Al-10Ti and Al-10Ti-2SiC samples as compared to Al-5Ti sample, clearly showing that the amount of $TiAl_3$ phase has increased by increasing the Titanium content in Aluminum matrix.

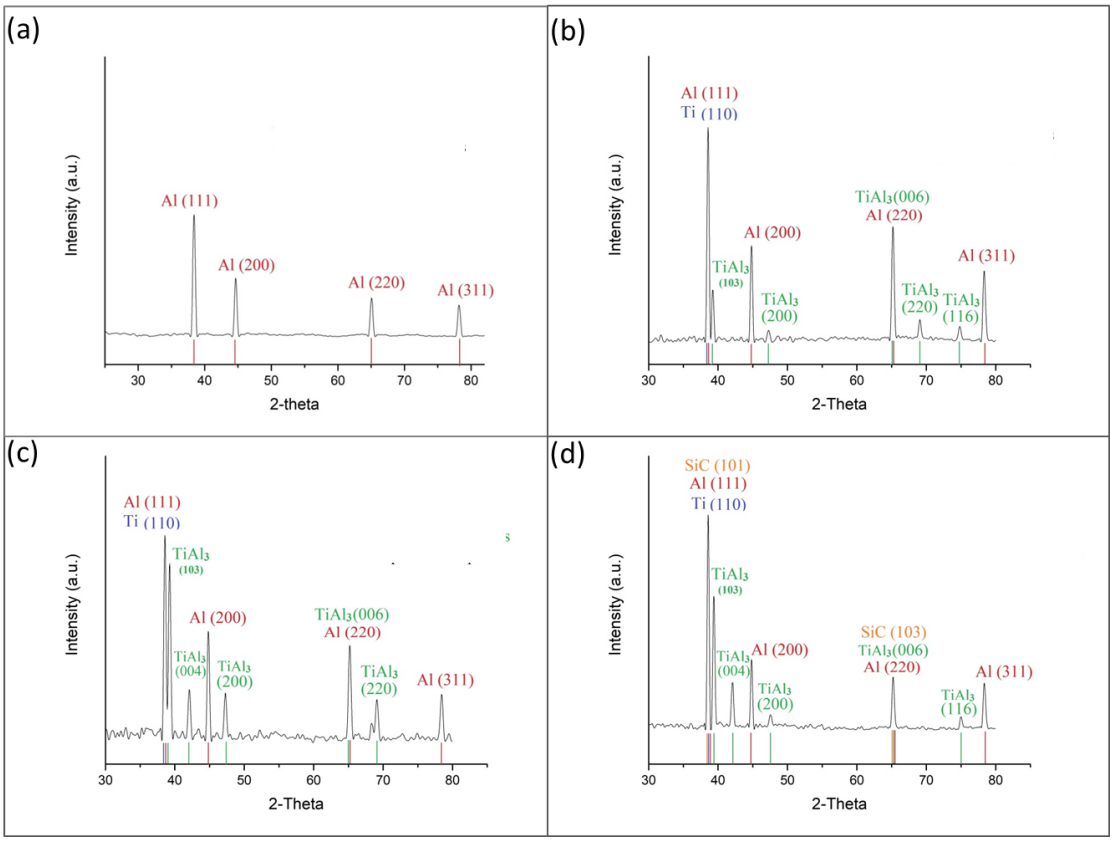


**Figure 7.** XRD of sintered alloy samples with indices (a) Pure Al; (b) Al-5%Ti; (c) Al-10%Ti; (d) Al-10%Ti-2% SiC.

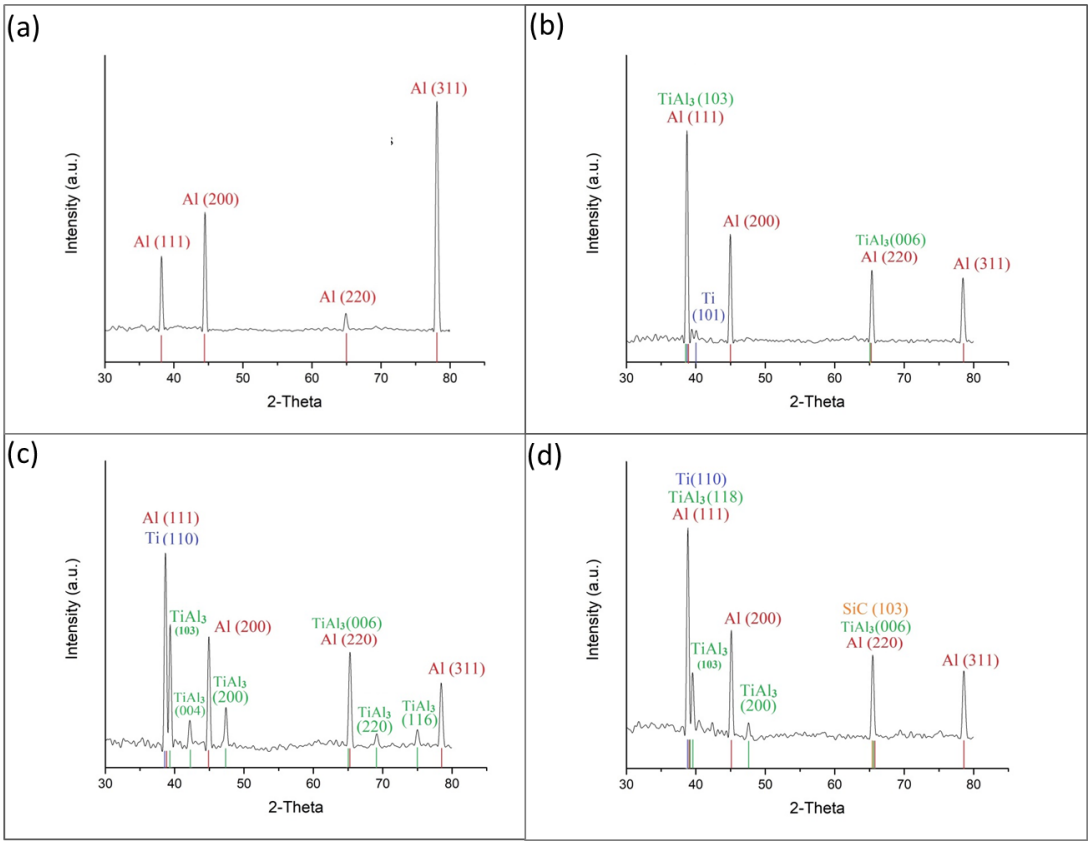


**Figure 8.** XRD of arc melted alloy samples with indices (a) Pure Al; (b) Al-5%Ti; (c) Al-10%Ti; (d) Al-10%Ti-2% SiC.

To quantify the phases indicated in the XRD patterns of arc melted and sintered alloys, the reference intensity ratio (RIR) quantification analysis was used. For arc melted alloys, the percentage of $TiAl_3$ was found to be 18%, 31%, and 33% for Al-5Ti, Al-10Ti, and Al-10Ti-2SiC respectively. For sintered alloys, the percentages of $TiAl_3$ was measured as 5%, 32%, 27% for above-mentioned compositions respectively. The remaining percentage is of Al in both arc melted and sintered alloys. The XRD phase analysis shows that the percentage of $TiAl_3$ is increasing with increasing content of Ti in the Al matrix. The SiC carbide was not detected in XRD diffractograms because of its smaller content.

### 3.4. Microhardness

Figure 9 represents the micro Vickers hardness values of sintered and arc melted samples. In the case of sintered samples, the average hardness values of pure Al were found as 19 HV. A little increment in Vickers hardness from 19 HV to 22 HV was observed with the addition of 5% Ti in Al.

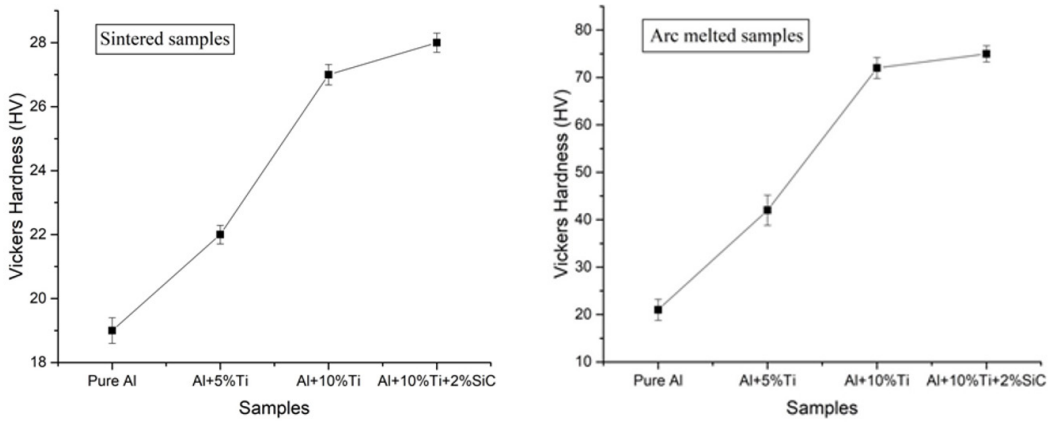


**Figure 9.** Separate hardness graphs with error bars of alloy samples fabricated through powder metallurgy and arc melting.

This could be due to the formation of a small amount of intermetallic compound $TiAl_3$ and solid solution strengthening effect due to little solubility of Ti in Al. Further 10% addition of Ti in Al increased the hardness value up to 27 HV which is a result of more intermetallic phase formation in the sample as confirmed from XRD analysis. The strengthening in this composition range (i.e. 5-10% Ti in Al) is a result of dispersion of intermetallic $TiAl_3$ phase which generates strain field in the Al matrix which in turn increases the hardness. As solid solubility of Ti in Al is very limited (about 1%), so solid solution strengthening effect is negligible and dispersion of intermetallic $TiA_{l3}$ phase is responsible for the increase in the hardness of Al-10Ti as compared to pure Al. A very small ceramic reinforcement i.e. 2% of SiC in Al-10Ti-2SiC further enhanced the hardness up to 28 HV.

As for the alloy samples fabricated through arc melting, hardness trend was found similar to alloys developed by powder metallurgy route, a gradual increasing trend in hardness values with an increasing amount of Ti was observed. However, hardness values were found much higher than sintered alloy samples. Average hardness of the pure Al sample was 21 HV. Alloy sample with 5%Ti resulted in 42 HV which was exactly double of pure Al sample. Hardness value of 72 HV was achieved for the sample with 10%Ti. Highest value achieved was75 HV for Al-10Ti-2SiC.

Figure 9 shows an increase in hardness for sintered samples is less than arc melted samples. SEM micrographs (Figure 5 and 6) give a better understanding of these results. Alloy formed in Al-Ti system generally acquire high hardness values due to the formation of hard and uniformly dispersed intermetallic phases. SEM Images show that intermetallic phase $TiAl_3$ is more uniformly dispersed throughout the alloy matrix in arc melted samples as compared to sintered samples thus causing higher hardness values. It was also difficult to control the porosity in powdered samples than arc melted samples, so hardness trend of arc melted samples were found similar to powder metallurgy route but the hardness values were small for samples developed by powder metallurgy route than with arc melting method. These results show that the addition of Titanium, as well as SiC, are effective in improving the strength of aluminum due to precipitation hardening due to the formation of $TiAl_3$ phase, solid solution strengthening effect and dispersion of SiC phase in an aluminum matrix of these alloy compositions.

## 4. Conclusions

Two sets of test samples based on Al and Ti metals and SiC reinforcement were prepared using powder metallurgy and arc melting routes. Reasonable densification was found in all test samples synthesized via powder metallurgy technique. Scanning electron microscopy of samples showed an overall uniform distribution of intermetallic phase in Al-Ti alloy for arc

melted samples as compared to sintered samples. Intermetallic phases were seen in the form of small islands in Al-matrix. In case of arc melted samples, flakes of intermetallic phase, uniformly dispersed in alloy matrix were seen. EDS and XRD analysis confirmed the presence of $TiAl_3$ intermetallic phase in the alloy samples. Specimens of both types displayed a gradual increment in hardness with the addition of 5 at.% and 10 at.% of Ti. A higher value of hardness was observed for Al-10Ti-2SiC ceramic reinforcement. In comparison, arc melted samples showed higher hardness values than sintered samples prepared by powder metallurgy route. These results verify that the alloy produced in the Al-Ti system provides better hardness aspects and these alloys are good option to replace heavier alloys for light weight and aerospace-related applications.

## Acknowledgements

Authors are thankful to the Higher Education Commission (HEC) Pakistan for provision of research funding under the National Research Program for Universities (NRPU) project # 20-3844/R&D/HEC/14. Authors also acknowledge the support of Materials Science and Engineering Department, Institute of Space Technology (IST) and Faculty of Chemical and Materials Engineering (FCME), Ghulam Ishaq Khan Institute (GIKI) Pakistan. Authors are also thankful to Dr. Zameer Abbas for his support during the experimentation. Authors are also thankful to engineer Luqman Hashmi for his help in the revision of this manuscript.

## References

[1] Hirsch J. Recent development in aluminium for automotive applications. Transactions of Nonferrous Metals Society of China. 2014;24(7):1995-2002. http://dx.doi.org/10.1016/S1003-6326(14)63305-7.

[2] Leyens C. Titanium alloys for aerospace applications. In: Leyens C, Peter M. Titanium and titanium alloys: fundamentals and applications. Weinheim: Wiley-VCH Verlag GmbH & Co. KgaA; 2003. p. 333-349.

[3] Campbell FC. Lightweight materials: understanding the basics. Materials Park: ASM International; 2012. Introduction and uses of lightweight materials; p. 1-29.

[4] Lumley RN. Application of modern aluminum alloys to aircraft. In: Lumley R. Fundamentals of aluminium metallurgy: production, processing and applications. 1st ed. Cambridge: Woodhead Publishing; 2011. p. 747-783. http://dx.doi.org/10.1533/9780857090256.

[5] Wadood A, Yamabe-Mitarai Y. Silver- and Zirconium-added ternary and quaternary TiAu based high temperature shape memory alloys. Journal of Alloys and Compounds. 2015;646:1172-1177. http://dx.doi.org/10.1016/j.jallcom.2015.06.057.

[6] Tisza M, Czinege I. Comparative study of the application of steels and aluminum in lightweight production of automotive parts. International Journal of Lightweight Materials and Manufacture. 2018;1(4):229-238. http://dx.doi.org/10.1016/j.ijlmm.2018.09.001.

[7] Jenkins M. Good Vibrations: materials swing into action. Materials World. 2000;8(6):11-13.

[8] Wongkeo W, Chaipanich A. Compressive strength, microstructure and thermal analysis of autoclaved and air cured structural lightweight concrete made with coal bottom ash and silica fume. Materials Science and Engineering A. 2010;527(16-17):3676-3684. http://dx.doi.org/10.1016/j.msea.2010.01.089.

[9] Staiger MP, Pietak AM, Huadmai J, Dias G. Magnesium and its alloys as orthopedic biomaterials: a review. Biomaterials. 2006;27(9):1728-1734. http://dx.doi.org/10.1016/j.biomaterials.2005.10.003. PMid:16246414.

[10] Nesper R. Bonding patterns in intermetallic compounds. Angewandte Chemie International. 1991;30:789-817. http://dx.doi.org/10.1002/anie.199107891.

[11] Kevorkijan V. Pressureless sintering and characterization of B4C, TiC and TiB2-particle-reinforced TiAl3-matrix composites. Materiali in Tehnologije. 2009;43:123-128.

[12] Zhang K, Li Z, Gao W. Hot corrosion behaviour of Ti-Al based intermetallics. Materials Letters. 2002;57(4):834-843. http://dx.doi.org/10.1016/S0167-577X(02)00882-0.

[13] Marketz WT, Fischer FD, Clemens H. Deformation mechanisms in TiAl intermetallics: experiments and modeling. International Journal of Plasticity. 2003;19(3):281-321. http://dx.doi.org/10.1016/S0749-6419(01)00036-5.

[14] Dimiduk D. Gamma titanium aluminide alloys: an assessment within the competition of aerospace structural materials. Materials Science and Engineering A. 1999;263(2):281-288. http://dx.doi.org/10.1016/S0921-5093(98)01158-7.

[15] Beygi R, Kazeminezhad M, Kokabi AH. Microstructural evolution and fracture behavior of friction-stir-welded Al-Cu laminated composites. Metallurgical and Materials Transactions. A, Physical Metallurgy and Materials Science. 2014;45(1):361-370. http://dx.doi.org/10.1007/s11661-013-1989-z.

[16] Batalu D, Coşmeleaţă G, Aloman A. Critical analysis of the Ti-Al phase diagrams. UPB Scientific Bulletin, Series B: Chemistry and Materials Science. 2006;68(4):77-90.

[17] Baker H. Alloy phase diagrams. In: ASM International. ASM handbook. Vol. 3. Materials Park: ASM International; 1992.

[18] Kim Y-W. Ordered intermetallic alloys, part III: gamma titanium aluminides. JOM. 1994;46(7):30-39. http://dx.doi.org/10.1007/BF03220745.

[19] Liu CT, Schneibel JH, Maziasz PJ, Wright JL, Easton DS. Tensile properties and fracture toughness of TiAl alloys with controlled microstructures. Intermetallics. 1996;4(6):429-440. http://dx.doi.org/10.1016/0966-9795(96)00047-7.

[20] Kastenhuber M, Rashkova B, Clemens H, Mayer S. Enhancement of creep properties and microstructural stability of intermetallic β-solidifying γ-TiAl based alloys. Intermetallics. 2015;63:19-26. http://dx.doi.org/10.1016/j.intermet.2015.03.017.

[21] Lin N, Zou J, Li M, Guo J, Ma Y, Wang Z, et al. Review on improvements in surface performance of TiAl-based alloys by double glow plasma surface alloying tecnology. Reviews on Advanced Materials Science. 2016;44:238-256.

[22] Djanarthany S, Viala J-C, Bouix J. An overview of intermetallic matrix composites based on Ti3Al and TiAl. Materials Chemistry and Physics. 2011;8:301-319. http://dx.doi.org/10.1515/secm.1999.8.5.275.

[23] Tetsui T, Shindo K, Kobayashi S, Takeyama M. A newly developed hot worked TiAl alloy for blades and structural components. Scripta Materialia. 2002;47(6):399-403. http://dx.doi.org/10.1016/S1359-6462(02)00158-6.

[24] Appel F, Brossmann U, Christoph U, Eggert S, Janschek P, Lorenz U, et al. Recent progress in the development of gamma titanium aluminide alloys. Advanced Engineering Materials. 2000;2(11):699-720. http://dx.doi.org/10.1002/1527-2648(200011)2:11<699::AID-ADEM699>3.0.CO;2-J.

[25] Wang PY, Li HJ, Qi LH, Zeng XH, Zuo HS. Synthesis of Al-TiAl3compound by reactive deposition of molten Al droplets and Ti powders. Prog. Nat. Sci. Mater. Int. 2011;21(2):153-158. http://dx.doi.org/10.1016/S1002-0071(12)60049-5.

[26] Cao WB, Kirihara S, Miyamoto Y, Matsuura K, Kudoh M. Development of freeform fabrication method for Ti-Al-Ni intermetallics. Intermetallics. 2002;10(9):879-885. http://dx.doi.org/10.1016/S0966-9795(02)00085-7.

[27] Yener T, Okumus SC, Zeytin S. In situ formation of Ti-TiAl<inf>3</inf> metallic-intermetallic composite by electric current activated sintering method. Acta Physica Polonica A. 2015;127(4):917-920. http://dx.doi.org/10.12693/APhysPolA.127.917.

[28] Yue YL, Gong YS, Shen Q, Zhang LM. Combustion synthesis of γ-TiAl intermetallic compound powder. Key Engineering Materials. 2003;249:467-470. http://dx.doi.org/10.4028/www.scientific.net/KEM.249.467.